Journal of Sustainable Metallurgy (2025) 11:4334–4346
https://doi.org/10.1007/s40831-025-01253-6

RESEARCH ARTICLE

Efficient Recovery of Platinum and Palladium by Fixed-Bed Column Adsorption Using Acylthiourea- and Amine-Modified Silica

Malehlogonolo R. R. Mphahlele[1] · Alseno K. Mosai[2] · Hlanganani Tutu[1] · Izak A. Kotzé[1]

Received: 26 June 2025 / Accepted: 26 August 2025 / Published online: 17 September 2025

Abstract

The rising demand and limited natural reserves of platinum group metals (PGMs) have intensified the need for sustainable recovery from secondary sources. This study investigates the continuous fixed-bed column adsorption of platinum (Pt) and palladium (Pd) from aqueous solutions using silica-anchored acylthiourea and amine-modified adsorbents. Adsorption experiments were performed at pH 2 and a flow rate of 2.00 mL/min, with variations in bed height and metal concentration to optimise recovery. Among the four adsorbents tested, DTMSP-BT-SG exhibited the highest adsorption capacities, with Thomas model-derived values reaching 470.67 mg/g for Pt and 382.19 mg/g for Pd. Increasing bed height and metal concentration enhanced both breakthrough capacity and the volume of solution treated, with up to 4775 bed volumes processed. Comparison with batch-mode adsorption revealed that, although equilibrium was achieved more rapidly in batch systems, column mode enabled significantly higher treatment volumes and yielded higher capacities. Breakthrough data were best described by the Thomas and Yoon–Nelson models ($R^2 > 0.90$), while the Bohart–Adams model was less predictive across the full breakthrough profile. The findings confirm the superior performance of acylthiourea-based adsorbents, particularly DTMSP-BT-SG, in large-scale continuous recovery of Pt and Pd from industrial and mining wastewater.

The contributing editor for this article was Kuniaki Murase.

✉ Izak A. Kotzé
Izak.Kotze@wits.ac.za

[1] School of Chemistry, Molecular Sciences Institute, University of the Witwatersrand, Private Bag X3, WITS, Johannesburg 2050, South Africa

[2] Department of Chemistry, Faculty of Natural and Agricultural Sciences, University of Pretoria, Lynwood Road, Pretoria 0002, South Africa

Graphical Abstract

Silica anchored acylthiourea and amine adsorbents enabled efficient continuous recovery of platinum and palladium in fixed-bed columns. These systems processed much larger solution volumes than batch methods, demonstrating strong potential for industrial scale applications.

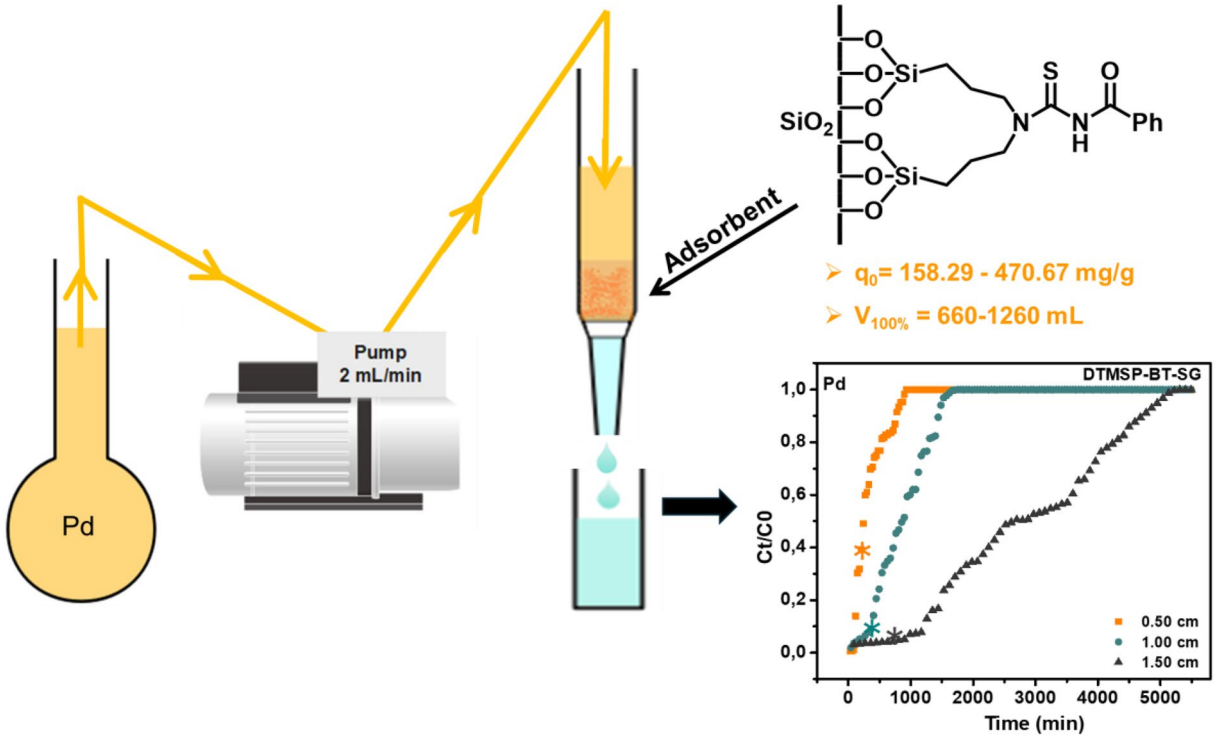

Keywords Fixed-bed column adsorption · Breakthrough curve modelling · Acylthiourea-functionalised silica · Platinum group metals (PGMs)

Introduction

Platinum (Pt) and palladium (Pd), owing to their unique physicochemical properties, play indispensable roles across a broad spectrum of scientific and industrial applications. These include catalytic converters in the automotive industry, electronics, fuel cells, jewellery, and medicine [1–5]. The global push for cleaner energy and stricter environmental regulations has further accelerated the demand for Pt and Pd, particularly in catalytic and hydrogen-based technologies [3–5].

However, the natural occurrence of platinum group metal (PGM) ores is scarce, and their extraction involves costly, energy-intensive processes. This has resulted in a widening gap between industrial demand and natural supply, prompting urgent interest in alternative, sustainable recovery strategies [5–7]. Among these, the recycling of secondary sources, such as electronic waste, spent automotive catalysts, and PGM-laden industrial effluents, offers a viable and environmentally responsible solution [6–10]. Nonetheless, these waste streams often pose ecological hazards, necessitating recovery methods that are not only efficient and selective, but also cost-effective and environmentally benign [6, 11, 12].

Several recovery techniques have been explored, including solvent extraction, precipitation, ion exchange, and adsorption [12–16]. Among them, adsorption stands out for its operational simplicity, high efficiency, low cost, and minimal waste generation [12–15]. Adsorption can be executed in batch or continuous (fixed-bed) modes depending on application scale.

In recent years, several adsorbent materials have been reported for Pd recovery, including ionic liquid–functionalised mesoporous silica composites, metal-doped inorganic matrices, and organically modified silicates [16, 17]. These systems highlight the importance of surface chemistry, ligand functionality, and structural properties in governing sorption performance. Such studies offer a broader context for evaluating our silica-anchored acylthiourea and amine-based adsorbents.

Batch adsorption is widely used for laboratory-scale removal of metal ions and is valued for its flexibility in optimising parameters such as pH, concentration, temperature, and contact time [19–22]. However, its limitations in throughput and scalability render it less suitable for industrial applications [22, 23].

Fixed-bed column adsorption, by contrast, offers a scalable and continuous approach for treating larger volumes of wastewater [23–25]. In this mode, the solution is passed through a column packed with adsorbent material, facilitating high-throughput recovery while maintaining selectivity and efficiency.

In our previous studies, we developed novel silica-anchored acylthiourea adsorbents and demonstrated their high efficiency and selectivity for Pt and Pd recovery in batch systems [26, 27]. These materials significantly outperformed comparable amine-functionalised silica gels under simulated refinery conditions. Building on this success, the current study extends the investigation to fixed-bed column systems to evaluate the scalability and industrial potential of these adsorbents.

Herein, we examine the performance of four functionalised silica gel adsorbents, two bearing acylthiourea ligands and two with amine groups, for continuous recovery of Pt and Pd from aqueous solutions. As part of a staged evaluation, this study focuses on adsorption performance in fixed-bed column systems, while recovery and adsorbent reusability investigations are being undertaken separately to inform full process optimisation. We assess the effects of bed height and influent concentration on adsorption performance and apply kinetic models (Thomas, Yoon–Nelson, Bohart–Adams) to describe the breakthrough dynamics. The findings offer insights into the practical implementation of these materials for large-scale recovery of PGMs from wastewater and secondary industrial streams.

Experimental

Reagents and Apparatus

All reagents were of analytical grade and used without further purification. Benzoyl chloride, potassium thiocyanate (KSCN), bis(3-trimethoxysilylpropyl)amine (BTMSPA), (3-aminopropyl)triethoxysilane (APTES), and silica gel (Davisil Grade 710, pore size 50–76 Å) were purchased from Sigma-Aldrich, South Africa. Stock solutions of Pt and Pd (1000 mg L^{-1} in 5% w/w HCl) were refrigerated at 4 °C until use. The pH of the working solutions was adjusted using 0.01 mol L^{-1} of HCl or NaOH.

The synthesis of the acylthiourea ligands, N,N-di(trimethoxysilylpropyl)-N'-benzoylthiourea (DTMSP-BT) and N-triethoxysilylpropyl-N'-benzoylthiourea (TESP-BT), followed procedures previously reported by our group [26, 27]. These ligands were immobilised onto silica gel to produce the functionalised adsorbents, alongside the corresponding amine-modified silica derivatives (BTMSPA-SG and APTES-SG). Detailed structural characterisation of the ligands and adsorbents has also been published previously, with structures shown in online supplementary material Fig. S1 [26, 27]. This study focuses on evaluating these materials in fixed-bed column adsorption experiments for the recovery of Pt and Pd from aqueous solutions.

Fixed-Bed Column Adsorption

Column experiments were conducted using borosilicate glass columns (4.00 mm internal diameter, 150.00 mm height) packed with known masses (22.5, 40.0, and 67.0 mg) of each adsorbent, corresponding to bed heights of 0.50, 1.00, and 1.50 cm, respectively. A layer of glass wool was used at both ends to support the adsorbent bed. The packed columns were connected to a Masterflex peristaltic pump (Cole-Parmer, USA) to maintain a constant downflow rate of 2.00 mL min^{-1}.

Metal ion solutions (3, 5, or 10 mg L^{-1} of Pt or Pd) were passed through the columns at pH 2. Each metal was tested separately; Pt and Pd solutions were prepared and run in independent column experiments. Stock solutions were based on 1000 mg L^{-1} standards in 5% (w/w) HCl. The chloride ion concentration in the test solution was approximately 1.41 mol L^{-1}, and the ionic strength, accounting for full dissociation of HCl and the presence of $H_2[PtCl_6]$ or $H_2[PdCl_4]$, was estimated at ~ 1.43 mol L^{-1}.

Effluent was collected in 20 mL aliquots at regular intervals, and the time required for each collection was recorded to calculate flow stability. The metal concentrations in the effluent were quantified using inductively coupled plasma optical emission spectroscopy (ICP-OES, Spectro Genesis, Germany). Column operation was continued until the effluent concentration (C_t) equalled the influent concentration (C_0), indicating adsorbent saturation.

An illustrative schematic of the fixed-bed setup is presented in Fig. 1.

Breakthrough Analysis

The performance of continuous adsorption in a fixed-bed column is typically described using breakthrough curves [15, 25]. These curves plot the effluent-to-influent concentration ratio (C_t/C_0) as a function of time (min) or effluent volume (mL) (Fig. 2) [28, 29]. They provide crucial information about the breakthrough point, defined as the moment when the adsorbate begins to appear in the effluent [28–30]. This point can be arbitrarily defined within the range of 5–90% of the influent concentration, though a Ct/C_0 value of 0.50

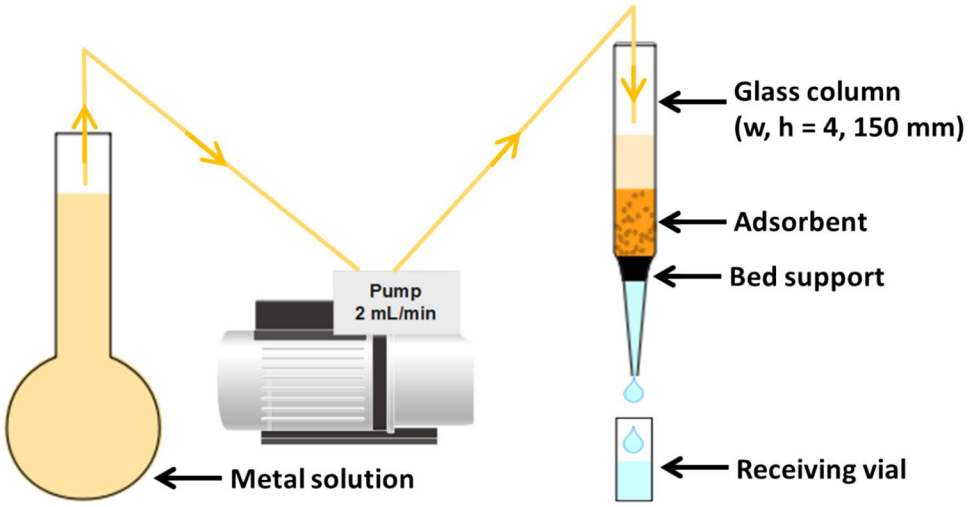

Fig. 1 Illustration for fixed-bed column adsorption

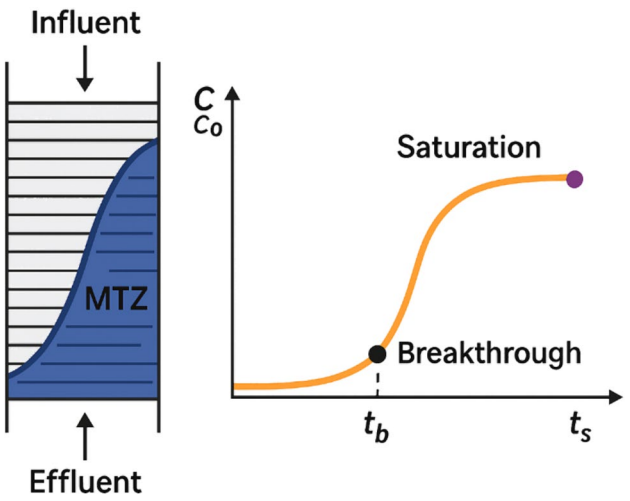

Fig. 2 Illustration of breakthrough curve (adapted with permission from Ref. [29])

(50%) is often used in industrial applications and is adopted in this study [20, 22, 30].

To better understand breakthrough behaviour and the fixed-bed process, the concept of the mass transfer zone (MTZ), also referred to as the primary sorption zone (PSZ), is introduced [22, 28, 29]. The MTZ represents the region within the adsorbent bed where active adsorption takes place [28, 29]. Initially, when the influent is introduced, the upper portion of the bed comes into contact with the metal ions, and the effluent contains negligible metal concentrations ($Ct/C_0 \approx 0$) [22, 29–31]. As adsorption progresses, this upper section becomes saturated, and the MTZ migrates downward to the unsaturated regions of the bed [22, 29].

This downward movement of the MTZ results in a gradual increase in the effluent concentration, as indicated by a rising Ct/C_0 ratio (e.g., $C_t/C_0 = 0.25$, 0.50, etc.) [29–31]. The operating limit of the column is typically reached when C_t/C_0 equals 0.90, beyond which the adsorptive performance declines sharply [22, 29–31]. When Ct/C_0 reaches 1.0 (i.e., the effluent concentration equals the influent), the adsorbent is considered fully saturated or exhausted and must be replaced to sustain effective metal removal [29–31].

The breakthrough curve enables the calculation of several performance parameters, including the adsorbed metal amount at breakthrough, q (mg), breakthrough adsorption capacity, q_b (mg/g), bed volume processed (BV), and the adsorbent exhaustion rate (AER) [30–33].

Adsorbed metal amount (q)

$$q = \frac{Q}{1000}\int_{t=0}^{t=t_b} C_0 - C_t dt \tag{1}$$

Breakthrough adsorption capacity (q_b)

$$q_b = \frac{q}{m}, \tag{2}$$

where Q is the volumetric flow rate (mL/min), t_b is the breakthrough time (min), C_0 and C_t are the influent and effluent concentrations (mg/L), respectively, and m is the adsorbent bed mass (g).

Bed volume (BV) is a measure of the volume of solution treated relative to the volume of the adsorbent bed, providing insight into bed utilisation efficiency: [33]

$$BV = \frac{\text{volume of water treated at breakthrough point}(L)}{\text{volume of adsorbent bed}(L)} \tag{3}$$

Adsorbent exhaustion rate (AER) reflects how frequently the adsorbent must be replenished:

$$AER = \frac{\text{mass of adsorbent } (g)}{\text{volume of water treated}(L)} \tag{4}$$

A higher BV and a lower AER both indicate enhanced column performance and operational efficiency.

Breakthrough Curve Models

Mathematical models are frequently applied to interpret fixed-bed column adsorption data, enabling the prediction of adsorption behaviour under varying operating conditions. These models help elucidate the adsorption mechanism, surface properties, and the affinity between adsorbate and adsorbent [33–35]. Furthermore, they are essential tools in the design and optimisation of large-scale adsorption systems [31–33]. The three commonly used models for fixed-bed column analysis are the Thomas, Yoon–Nelson, and Bohart–Adams models [31–35].

The Thomas model is based on the Langmuir isotherm and assumes that the adsorption process follows second-order reversible kinetics and is controlled by mass transfer rather than chemical reaction [34–36]. This model is widely employed for performance estimation of fixed-bed systems.

The linearised Thomas model is given as:

$$\ln\left(\frac{C_0}{C_t}-1\right)=\frac{k_{\mathrm{Th}}q_0 m_{\mathrm{adsorbent}}}{Q}-k_{\mathrm{Th}}C_0 t, \tag{5}$$

where k_{Th} is the Thomas rate constant (L min^{-1} mg^{-1}), q_0 is the adsorption capacity (mg/g), m is the mass of adsorbent (g), Q is the influent flow rate (mL/min), C_0 and C_t are the influent and effluent concentrations (mg/L) and t is the flow time (min).

From the slope and intercept of the linear plot of ln (C_0/C_t-1) vs. time (t) the constants k_{Th} and q_0 can be determined.

The Yoon–Nelson model is a simplified approach that assumes the probability of adsorbate breakthrough is proportional to the probability of adsorbate adsorption. It does not require detailed information about the adsorbent or the adsorbate [31, 35]. This model assumes that the reduction in adsorption probability is directly proportional to the adsorption of the adsorbate and breakthrough on the adsorbent [31–35]. The Yoon–Nelson model provides information on the breakthrough rate and can be used to determine the time required to reach 50% breakthrough [23, 31]. This model is expressed as:

$$\ln\left(\frac{C_0}{C_0-C_t}\right)=k_{\mathrm{YN}}t-\tau k_{\mathrm{YN}}, \tag{6}$$

where k_{YN} is the Yoon–Nelson kinetic constant (1/min) and τ is the time required to reach 50% breakthrough (min).

From the linear plot of ln $(C_0/(C_0-C_t))$ vs. t, the values of k_{YN} and τ can be obtained [31].

The Bohart–Adams model is typically used to describe the initial part of the breakthrough curve ($C_t/C_0<0.5$), and assumes that adsorption rate is proportional to the residual capacity of the adsorbent and the adsorbate concentration [30–36].

The model is given by:

$$\ln\left(\frac{C_t}{C_0}\right)=k_{\mathrm{AB}}C_0 t-\frac{k_{\mathrm{AB}}N_0 Z}{V}, \tag{7}$$

where k_{AB} is the Bohart–Adams rate constant (L min^{-1} mg^{-1}), N_0 is the saturation concentration (mg/L), Z is the bed height (cm), V is the linear velocity of the solution (cm/min) and t is the time (min).

Here, V is calculated by dividing the volumetric flow rate (cm^3/min) by the cross-sectional area of the column (cm^2) [36].

Results and Discussion

Effect of Bed Height

The effect of bed height on the adsorption performance of DTMSP-BT-SG was investigated at a constant flow rate of 2.00 mL/min, an initial metal concentration of 10.0 mg/L, and solution pH 2. Bed heights of 0.50, 1.00, and 1.50 cm (corresponding to adsorbent masses of 22.5, 40.0, and 67.0 mg, respectively) were evaluated (Fig. 3).

The results revealed that increasing bed height led to a delayed breakthrough, indicating prolonged column operation. This trend can be attributed to the greater number of available active sites at higher bed heights, allowing for more extensive interaction between the adsorbate and the adsorbent [37, 38]. Consequently, the breakthrough adsorption capacities (q_b) increased with bed height, ranging from 68.86 to 242.60 mg/g for Pt and from 48.28 to 194.29 mg/g for Pd [6, 38].

Additionally, greater bed heights allowed for larger volumes of influent to be treated prior to breakthrough. The processed bed volumes (BV) increased from 3183 to 3714 (Pt) and 2546 to 3395 (Pd), as shown in Table 1. These findings confirm that increasing the adsorbent bed height enhances both the adsorptive capacity and column utilisation [38, 39].

Higher beds also promoted longer contact times between metal ions and the adsorbent, which improved mass transfer efficiency [38, 39]. This is reflected in the extended exhaustion times ($T_{100\%}$), which ranged from 1050 to 5670 min for Pt and from 990 to 5310 min for Pd.

Breakthrough curves corresponding to higher bed heights exhibited broader mass transfer zones (MTZs) and more gradual slopes, indicative of improved adsorption dynamics and delayed saturation [38, 39].

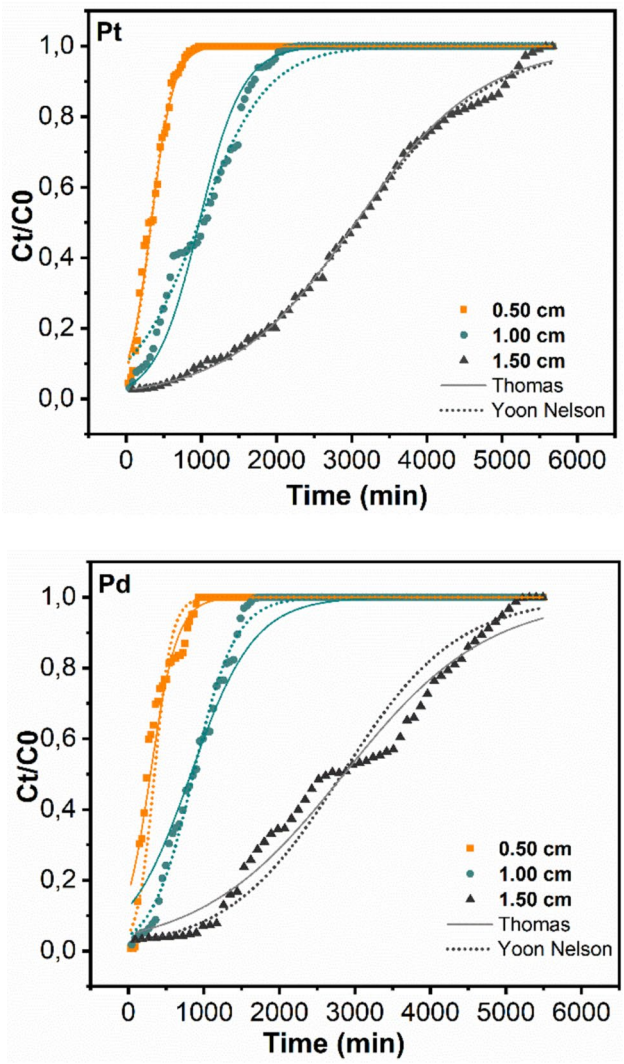

Fig. 3 Effect of bed height on the adsorption of **a** Pt and **b** Pd by DTMSP-BT-SG (initial concentration: 10.0 mg/L; flow rate: 2.00 mL/min; pH 2)

Empty Bed Contact Time (EBCT)

The empty bed contact time (EBCT) also referred to as bed service time, is a critical design parameter for evaluating the efficiency of fixed-bed adsorption systems [19, 39, 40]. EBCT represents the theoretical time the influent solution remains in contact with the adsorbent bed under ideal plug flow conditions. It is calculated using the following relationship:

$$EBCT = \frac{V_b}{Q} \tag{5}$$

In this study, the flow rate was constant at 2.00 mL/min (0.033 mL/s), and the bed volume increased proportionally with adsorbent mass. The calculated EBCT values are presented in Table 1 and ranged from 5.65 to 50.88 s as the bed height increased from 0.50 cm to 1.50 cm.

This increase in EBCT with bed height indicates longer residence times of the metal-laden solution within the column. The extended contact duration enhances the probability of metal ion interaction with active sites on the adsorbent, thereby improving overall adsorption performance. This is consistent with the observed increases in breakthrough capacity (q_b), exhaustion time ($T_{100\%}$), and bed volume processed (BV) at higher bed heights.

Furthermore, a higher EBCT corresponds to a broader mass transfer zone (MTZ), which is reflected in the more gradual slope of the breakthrough curves. This behaviour is favourable for continuous column operation, as it maximises metal recovery before saturation is reached [40, 41].

In summary, the increase in EBCT with bed height directly correlates with enhanced column efficiency and is a key factor contributing to the improved performance observed at greater bed depths.

Table 1 Breakthrough parameters analysis of DTMSP-BT-SG

Parameters	q_b (mg/g)		BV		AER (g/L)		EBCT (sec)	$T_{100\%}$ (min)	
	Pt	Pd	Pt	Pd	Pt	Pd		Pt	Pd
Mass (mg)									
22.5	68.86	48.28	3183	2546	0.032	0.034	5.65	1050	990
40.0	131.87	95.42	3661	3024	0.040	0.051	16.98	2295	1800
67.0	242.60	194.29	3714	3395	0.053	0.057	50.88	5670	5310
Concentration (mg/L)									
3.0	59.78	55.56	4775	4775	0.028	0.028	5.65	1230	1200
5.0	68.86	48.28	3183	3183	0.034	0.030	5.65	1050	990
10.0	116.05	76.62	2865	1910	0.043	0.047	5.65	720	780

q_b is adsorption capacity at breakthrough; BV is bed volume processed; AER is rate of adsorbent exhaustion; EBCT is empty bed contact time; $T_{100\%}$ is time at adsorbent saturation.

Effect of Metal Concentration

The influence of initial metal concentration on the column adsorption performance of DTMSP-BT-SG was studied at a fixed-bed height of 0.50 cm (22.5 mg adsorbent), a constant flow rate of 2.00 mL/min, and solution pH 2. Metal concentrations of 3.0, 5.0, and 10.0 mg/L were evaluated to simulate varying influent conditions (Fig. 4).

The breakthrough curves demonstrated that higher influent concentrations resulted in shorter breakthrough and exhaustion times. For Pt, the time to complete saturation ($T_{100\%}$) decreased from 1230 to 720 min as the concentration increased from 3.0 to 10.0 mg/L. Similarly, for Pd, $T_{100\%}$ decreased from 1200 to 780 min. This behaviour is attributed to the more rapid saturation of the adsorbent's active sites under higher metal loading conditions [39–43].

The breakthrough adsorption capacities (q_b) increased with rising influent concentration, due to the enhanced driving force for mass transfer and a higher concentration gradient between the solution and the adsorbent surface. This led to more efficient utilisation of the available active sites before breakthrough occurred.

However, the volume of solution treated before saturation decreased with increasing concentration, reflecting the faster exhaustion of the adsorbent bed. For instance, the bed volume (BV) decreased from 4775 to 2865 for Pt, and from 4775 to 1910 for Pd, as shown in Table 1.

The adsorbent exhaustion rate (AER) also increased with metal concentration, ranging from 0.028 to 0.043 g/L for Pt and from 0.028 to 0.047 g/L for Pd. A higher AER indicates more rapid consumption of the adsorbent, which may limit operational efficiency under high-concentration conditions.

In addition, the steepness of the breakthrough curves increased with metal concentration, indicative of a narrower mass transfer zone (MTZ) and reduced adsorption front stability. While this may lead to sharper breakthroughs, it also signifies higher adsorption rates during the initial stages of operation.

Overall, these findings confirm that while elevated metal concentrations enhance adsorption capacity, they also accelerate bed saturation and reduce operational time, necessitating careful optimisation in continuous treatment systems [32, 33, 40–43].

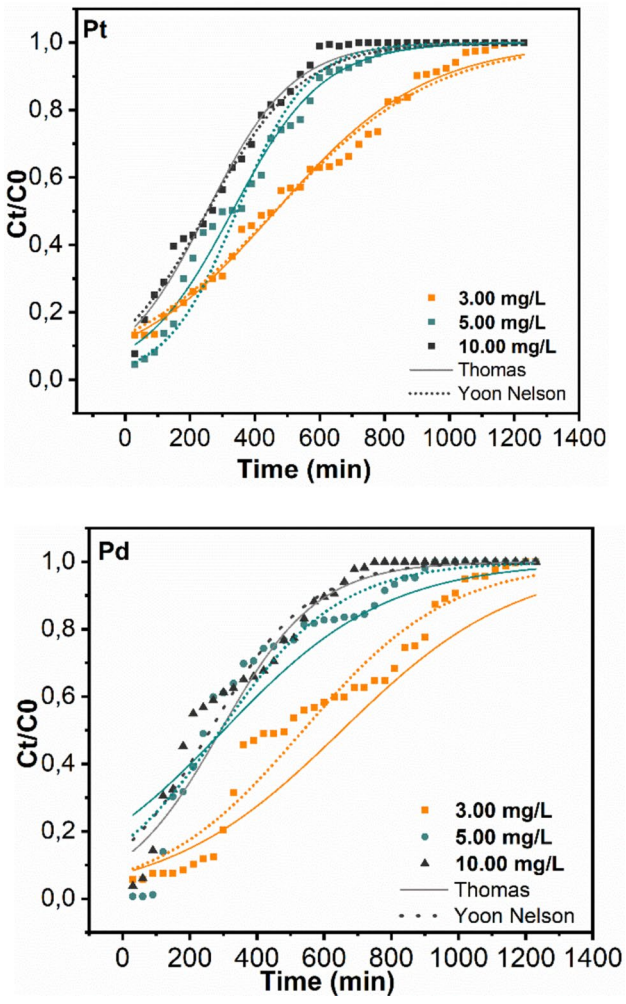

Fig. 4 Effect of influent metal concentration on the adsorption of **a** Pt and **b** Pd by DTMSP-BT-SG (bed height, 0.50 cm; flow rate, 2.00 mL/min; pH 2)

Comparing Efficiency of Batch vs. Column Adsorption

To assess the relative effectiveness of batch and fixed-bed column adsorption modes for Pt and Pd recovery, comparative evaluation was performed using previously reported batch data for DTMSP-BT-SG under identical conditions of pH, concentration, and temperature. The theoretical saturation volumes, derived from batch-mode adsorption capacities, were contrasted with the experimentally observed values in the column mode.

As presented in Table S2, the volume of solution treated at full saturation in column mode ($V_{100\%}$ ranged from 480 to 1260 mL) significantly exceeded the theoretical volume predicted from batch capacities ($V_{100\%}$ = 67–650 mL). This finding underscores the enhanced operational capacity and throughput of the column system, particularly under continuous flow conditions. Chowdhury et al. have noted that in batch mode, the adsorbent remains in static contact with a limited solution volume, whereas in column mode, continuous introduction of fresh influent allows for more efficient utilisation of active sites through progressive loading along the bed profile [20, 22, 29, 42].

In batch mode, quantitative extraction (> 99%) of Pt and Pd was achieved within 3 h [26, 27]. In contrast, in column studies, the corresponding saturation point, based on breakthrough analysis and predicted from batch-derived

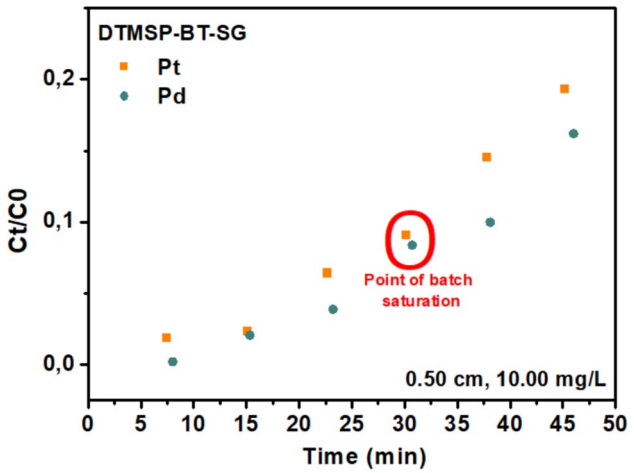

Fig. 5 Adsorption of Pt and Pd by DTMSP-BT-SG illustrating the expected saturation point based on batch mode capacities (bed-height, 0.50 cm; concentration, 10 mg/L; flow rate = 2.00 mL/min, pH 2)

capacities, occurred within 30 min (Fig. 5), indicating that the adsorbent retained considerable residual capacity beyond the batch-equivalent threshold.

Although the empty bed contact time (EBCT) in column mode was shorter (5.65 s) compared to batch contact durations, the overall breakthrough time ($T_{100\%}$ = 720–5670 min) was considerably extended. This slower kinetics in column mode is attributable to the continual supply of fresh metal solution, which gradually saturates the adsorbent bed while maintaining dynamic equilibrium [15, 22, 29, 42, 43]. The result is a substantially greater treatment volume per mass of adsorbent, as evidenced by the high bed volumes processed (up to 4775 BV).

It should be noted that column experiments were conducted intermittently, with operational pauses introduced overnight. These interruptions likely contributed to the non-uniformities observed in the breakthrough curves, manifesting as minor discontinuities or inflection points [39]. Nonetheless, the adsorbents maintained excellent performance, indicating robust stability under start-stop conditions.

In summary, while batch adsorption offers rapid metal extraction and easier parameter control, fixed-bed column mode demonstrates superior throughput, greater capacity utilisation, and operational scalability, making it a more practical option for continuous and large-scale PGM recovery applications.

Comparing Adsorption of Pt and Pd by DTMSP-BT-SG, TESP-BT-SG, BTMSPA-SG, and APTES-SG

To evaluate the comparative performance of all four adsorbents, additional fixed-bed column experiments were

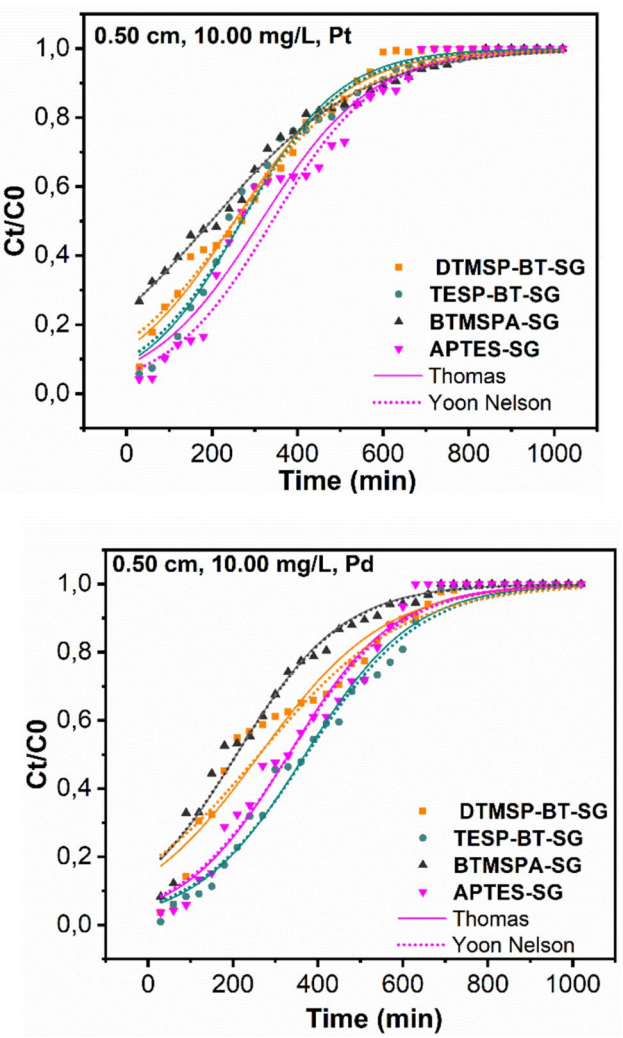

Fig. 6 Fixed-bed adsorption of Pt and Pd by DTMSP-BT-SG, TESP-BT-SG, BTMSPA-SG, and APTES-SG (flow rate: 2.00 mL/min, pH 2)

conducted using DTMSP-BT-SG, TESP-BT-SG, BTMSPA-SG, and APTES-SG under identical conditions: solution pH 2, flow rate 2.00 mL/min, bed height 0.50 cm (22.5 mg), and initial metal concentration of 10 mg/L (Fig. 6).

The breakthrough data (Table S3) revealed variations in breakthrough times (t_b) and total volumes treated. The breakthrough times ranged from 180 to 270 min, and the corresponding treated volumes spanned 120–220 mL, depending on the adsorbent and metal species.

Among the adsorbents tested, APTES-SG exhibited the highest adsorption capacity at breakthrough, indicating enhanced affinity for both Pt and Pd under these conditions. BTMSPA-SG on the other hand recorded the lowest adsorption capacities, consistent with the slower adsorption kinetics and lower ligand loading previously reported in batch studies [26, 27].

At complete saturation ($T_{100\%}$), the treated solution volumes ranged between 420 and 660 mL for the different adsorbents. These values exceeded the theoretical volumes predicted from batch-mode capacities (Table S2), further affirming the practical advantages of fixed-bed column operation in continuous applications.

The observed trends in performance are consistent with the structural and functional differences among the adsorbents. The acylthiourea-functionalised adsorbents (DTMSP-BT-SG and TESP-BT-SG) displayed comparable and superior adsorption efficiencies across both metals. This is attributed to the presence of multiple donor atoms (N, O, S), which enhance complexation and selectivity for soft metal ions such as Pt(IV) and Pd(II). The amine-functionalised adsorbents showed divergent behaviour. While APTES-SG performed favourably, BTMSPA-SG was less effective, likely due to steric hindrance and reduced accessibility of the amine sites.

In addition to adsorbent-specific effects, the difference in adsorption behaviour between Pt and Pd can also be attributed to their solution-phase speciation and coordination characteristics. In acidic chloride media, Pt(IV) exists as the kinetically inert [$PtCl_6$] [2-] complex, while Pd(II) forms the more labile [$PdCl_4$]$^{2-}$ species [43]. Pd(II), being smaller and more labile, adsorbs more rapidly but reaches saturation earlier. Pt(IV), due to its octahedral geometry and slow ligand exchange, binds more persistently to the donor atoms on the adsorbent surface, resulting in delayed breakthrough but prolonged retention.

These findings reinforce the significance of both ligand chemistry and surface functional group accessibility in determining column adsorption performance. The acylthiourea-based systems proved consistently superior, though the improved synthesis of APTES-SG yielded notable enhancements over BTMSPA-SG.

Breakthrough Curve Modelling

To quantitatively evaluate the adsorption performance and kinetics of the fixed-bed column system, the experimental data were fitted to three well-established models: Thomas, Yoon–Nelson, and Bohart–Adams (see the "Breakthrough Curve Models" section for model equations and assumptions). The model parameters, including adsorption capacities, kinetic constants, and breakthrough times, were determined using linear regression and are summarised in Tables 2 and 3.

Thomas Model

The Thomas model provided an excellent fit for both Pt and Pd adsorption, with correlation coefficients (R^2) ranging from 0.90 to 0.98. For DTMSP-BT-SG, the adsorption capacity (q_0) increased with both bed height and metal concentration, indicating enhanced metal uptake under conditions of greater adsorbent mass and higher driving force. For Pt, q_0 ranged from 158 to 470 mg/g and for Pd, q_0 ranged from 152 to 382 mg/g.

Among the four adsorbents tested, BTMSPA-SG exhibited the lowest q_0 values, in agreement with prior batch studies and reflecting its reduced active site availability [6, 39, 40]. TESP-BT-SG and APTES-SG also showed good conformity to the model, though the acylthiourea-functionalised materials consistently outperformed the amine-functionalised adsorbents.

These results demonstrate the applicability of the Thomas model in predicting column performance, especially in scaling adsorption capacity under varying conditions.

Yoon–Nelson Model

The Yoon–Nelson model also yielded high-quality fits across all experimental conditions, with R^2 values up to 0.98. The model's predictive parameter τ (the time to

Table 2 Fixed-bed column modelling adsorption data Pt recovery by DTMSP-BT-SG

Pt	Thomas			Yoon–Nelson			Bohart–Adams		
	$K_{Th}\times10^{-4}$	q_0	R^2	$k_{YN}\times10^{-3}$	T	R^2	$K_{AB}\times10^{-4}$	N_0	R^2
	L/min mg	mg /g		1/min	min		L/mg min	mg /L	
Mass (mg)									
22.5	17.01	159	0.93	8.79	345	0.93	4.85	127	0.71
40.0	6.73	239	0.93	3.48	938	0.93	2.32	152	0.81
67.0	2.32	471	0.98	1.20	3053	0.98	1.28	254	0.91
Concentration (mg/L)									
3.0	17.71	120	0.93	5.30	452	0.93	5.58	95	0.89
5.0	17.01	158	0.93	9.17	345	0.93	4.58	126	0.71
10.0	9.98	219	0.90	9.66	255	0.90	3.26	160	0.75

Table 3 Fixed-bed column modelling adsorption data of Pd recovery by DTMSP-BT-SG

Pd	Thomas			Yoon–Nelson			Bohart–Adams		
	$K_{Th} \times 10^{-4}$	q_0	R^2	$k_{YN} \times 10^{-3}$	T	R^2	$K_{AB} \times 10^{-4}$	N_0	R^2
	L/min mg	mg /g		1/min	min		L/mg min	mg /L	
Mass (mg)									
22.5	18.83	152	0.79	8.52	379	0.79	7.23	107.58	0.47
40.0	10.99	183	0.91	4.97	823	0.91	4.32	104.60	0.83
67.0	2.89	382	0.93	1.31	2829	0.93	1.49	213.11	0.86
Concentration (mg/L)									
3.0	20.96	134	0.93	5.82	542	0.93	8.70	87.07	0.81
5.0	19.11	152	0.78	8.65	378	0.78	7.23	107.58	0.47
10.0	9.16	245	0.87	8.77	287	0.87	3.03	190.22	0.63

50% breakthrough) correlated well with the actual breakthrough times, reinforcing the model's validity. The rate constant (k_{YN}) increased with metal concentration, due to accelerated saturation kinetics while τ increased with bed height, consistent with longer contact times and delayed breakthrough. The increase in k_{YN} with concentration is also attributed to an enhanced mass transfer gradient, resulting in improved bulk transfer rates under these conditions [6, 39, 43, 44].

Among the adsorbents, DTMSP-BT-SG displayed the highest τ, indicating superior adsorption retention. BTMSPA-SG, in contrast, exhibited the lowest τ, consistent with faster breakthrough and earlier exhaustion. These results confirm that the Yoon–Nelson model effectively captures breakthrough behaviour without requiring detailed structural information about the adsorbent.

Beyond fitting the current data, the model parameters provide predictive value for column design, enabling estimation of breakthrough time and bed saturation under different flow rates and concentrations. These outputs can inform scale-up strategies and operational planning in future process development.

Bohart–Adams Model

The Bohart–Adams model was applied to assess the initial breakthrough behaviour of Pt and Pd in the fixed-bed column system (Figs. S2 and S3). As discussed in the "Breakthrough Curve Models" section, this model is most applicable to the early phase of column operation, where the adsorbent bed is largely unsaturated. In this study, the Bohart–Adams model yielded only moderate correlation with the experimental data, with R^2 values ranging from 0.47 to 0.91 for Pd and 0.71 to 0.91 for Pt (Tables 2 and 3). These values were consistently lower than those obtained from the Thomas and Yoon–Nelson models, indicating that the Bohart–Adams model is less suited to describe the full breakthrough profile.

Separation Mechanism and Implications of Modelling

The adsorption profiles observed for Pt and Pd reflect the combined effects of mass transfer, surface affinity, and solution-phase speciation in acidic chloride media. In this environment, Pd(II) predominantly exists as the more labile $[PdCl_4]^{2-}$ complex, resulting in faster initial uptake and steeper breakthrough curves, but also earlier bed saturation. Pt(IV), in contrast, forms the kinetically inert $[PtCl_6]^{2-}$ species, leading to slower adsorption but stronger and more persistent binding. This behaviour is consistent with a chemisorption-dominated mechanism in which Pd achieves rapid site occupancy, whereas Pt is retained for longer due to slower ligand exchange.

The Thomas model parameters quantify maximum adsorption capacities and rate constants, providing insight into the extent and kinetics of metal uptake, while the Yoon–Nelson model offers robust estimates of breakthrough times and curve symmetry, which are valuable for process control. Taken together, these models validate the experimental profiles and clarify the adsorption–separation mechanism. They also provide predictive capability for scale-up, enabling operational parameters such as breakthrough time, bed saturation, and adsorbent lifetime to be estimated under varying flow rates and feed concentrations.

Conclusion

This study demonstrated the successful application of silica-anchored acylthiourea and amine adsorbents for the fixed-bed column recovery of platinum (Pt) and palladium (Pd) from aqueous solutions. Among the tested materials, DTMSP-BT-SG consistently outperformed the other adsorbents, displaying the highest adsorption capacities and longest breakthrough times under optimised conditions. Maximum adsorption was achieved at a bed height of 1.50 cm, influent concentration of 10 mg/L, pH 2, and

a constant flow rate of 2.00 mL/min. At these conditions, DTMSP-BT-SG exhibited breakthrough capacities of 242.60 mg/g (Pt) and 194.29 mg/g (Pd), with bed volumes processed up to 4775 and prolonged saturation times exceeding 5600 min.

Comparison with batch-mode performance revealed that although quantitative extraction occurred more rapidly in batch mode, the fixed-bed column offered superior throughput and capacity utilisation. The experimental volumes treated in column mode (up to 1260 mL) exceeded theoretical predictions based on batch capacities, indicating improved metal recovery per gram of adsorbent.

Breakthrough modelling using the Thomas and Yoon–Nelson models showed strong correlation with experimental data, with R^2 values above 0.90, confirming their reliability for describing column dynamics and estimating key parameters such as adsorption capacity and breakthrough time. The Bohart–Adams model, while less effective across the full breakthrough profile, provided useful comparative insights into initial adsorption kinetics.

Between the adsorbents, the acylthiourea-functionalised materials (DTMSP-BT-SG and TESP-BT-SG) outperformed the amine-functionalised alternatives (BTMSPA-SG and APTES-SG), owing to their multi-donor ligand systems and higher metal-binding affinity. However, APTES-SG showed notable improvement over BTMSPA-SG, highlighting the importance of ligand accessibility and loading.

The separation mechanism, as clarified in the "Separation Mechanism and Implications of Modelling" section, together with the predictive capability of the Thomas and Yoon–Nelson models, provides a strong basis for translating the laboratory-scale adsorption profiles into operational parameters for larger-scale recovery systems.

In conclusion, the findings establish silica-anchored acylthioureas, particularly DTMSP-BT-SG, as highly effective, selective, and scalable adsorbents for Pt and Pd recovery in fixed-bed systems. Their strong performance under simulated industrial conditions supports their potential for practical deployment in PGM recycling and wastewater remediation. Building on this foundation, future work will focus on developing elution protocols and assessing adsorbent reusability to enable long-term, continuous operation.

Supplementary Information The online version contains supplementary material available at https://doi.org/10.1007/s40831-025-01253-6.

Acknowledgements The authors thank the National Research Foundation (NRF (149354)) for financial support and the University of the Witwatersrand for the research facilities.

Funding Open access funding provided by University of the Witwatersrand.

Declarations

Conflict of interest On behalf of all authors, the corresponding author states that there is no conflict of interest.

References

1. Losev VN, Borodina EV, Buyko OV, Samoilo AS, Elsuf'ev E, Li M (2023) Highly selective adsorbents based on silica gel chemically modified with sulfur-containing groups of arched structure for preconcentration and determination of palladium (II) in products of processing of sulfide copper-nickel ore. Microchem J 195:109452. https://doi.org/10.1016/j.microc.2023.109452
2. Cosmin V, Mihailescu M, Negrea A, Giannin M, Mihaela C, Duteanu N, Negrea P, Vasile M (2020) Batch and fixed-bed column studies on palladium recovery from acidic solution by modified MgSiO3. Int J Environ Res Public Health 17(24):9500. https://doi.org/10.3390/ijerph17249500
3. Dong H, Zhao J, Chen J, Wu Y, Li B (2015) Recovery of platinum group metals from spent catalysts: a review. Int J Miner Process 145:108–113. https://doi.org/10.1016/j.minpro.2015.06.009
4. Wang Z, Kang SB, Won SW (2021) Selective adsorption of palladium (II) from aqueous solution using epichlorohydrin crosslinked polyethylenimine-chitin adsorbent: batch and column studies. J Environ Chem Eng 9(2):105058. https://doi.org/10.1016/j.jece.2021.105058
5. Kolbadinejad S, Ghaemi A (2023) Recovery and extraction of platinum from spent catalysts: a review. Case Stud Chem Environ Eng 7:100327. https://doi.org/10.1016/j.cscee.2023.100327
6. Khusnun NF, Hasan NS, Amalina I, Jalil AA, Firmansyah ML (2022) Enhanced recovery of palladium from an aqueous solution using an ionic liquid–mesoporous silica composite in batch and fixed-column studies. Ind Eng Chem Res 61(25):8634–8644. https://doi.org/10.1021/acs.iecr.2c01258
7. Mosai AK, Chimuka L, Cukrowska EM, Kotzé IA, Tutu H (2020) Batch and flow-through column adsorption study: recovery of Pt4+ from aqueous solutions by 3-aminopropyl(diethoxy)methylsilane functionalised zeolite (APDEMSFZ). Environ Dev Sustain 23(5):7041–7062. https://doi.org/10.1007/s10668-020-00903-x
8. Moleko-Boyce P, Makelane H, Ngayeka MZ, Tshentu ZR (2022) Recovery of platinum group metals from leach solutions of spent catalytic converters using custom-made resins. Minerals 12(3):361. https://doi.org/10.3390/min12030361
9. Yousif AM (2019) Recovery and then individual separation of platinum, palladium, and rhodium from spent car catalytic converters using hydrometallurgical technique followed by successive precipitation methods. J Chem 2019:1–7. https://doi.org/10.1155/2019/2318157
10. Yu C, Wu Z, Wang S, Zhong Q, Yang B, Xu J, Xiao K, Guibal E (2022) Batch sorption and fixed-bed elution for Pd recovery

using stable amine-functionalized melamine sponge. J Clean Prod 337:130475. https://doi.org/10.1016/j.jclepro.2022.130475
11. Masamvu MJ, Asmaa B, Belkacem M, Chitepo RM, Mohamed HB, Imene B, Boumediene H, Saleh A, Abdullah AA, Ghosh S, Chia CH, Sillanpaa M, Omirserik B, Hosseini-Bandegharaei A (2024) An overview on the key advantages and limitations of batch and dynamic modes of biosorption of metal ions. Chemosphere 357:142051. https://doi.org/10.1016/j.chemosphere.2024.142051
12. Asmaa B, Amine M, Elwakeel KZ, Hamza MF, Guibal E (2021) Recovery of heavy metal ions using magnetic glycine-modified chitosan—application to aqueous solutions and tailing leachate. Appl Sci 11(18):8377. https://doi.org/10.3390/app11188377
13. Sharma S, Wu CM, Koodali RT, Rajesh N (2016) An ionic liquid-mesoporous silica blend as a novel adsorbent for the adsorption and recovery of palladium ions, and its applications in continuous flow study and as an industrial catalyst. RSC Adv 6(32):26668–26678. https://doi.org/10.1039/c5ra26673d
14. Nagarjuna R, Sharma S, Rajesh N, Ganesan R (2017) Effective adsorption of precious metal palladium over polyethyleneimine-functionalized alumina nanopowder and its reusability as a catalyst for energy and environmental applications. ACS Omega 2(8):4494–4504. https://doi.org/10.1021/acsomega.7b00431
15. Mosai AK, Chimuka L, Cukrowska EM, Kotzé IA, Tutu H (2020) Recovery of Pt (IV) from aqueous solutions by spent brewer's yeast-functionalized zeolite (SBYFZ): a batch and column study. Environ Prog Sustain Energy. https://doi.org/10.1002/ep.13481
16. Pianowska K, Kluczka J, Benke G, Goc K, Malarz J, Ochmański M, Leszczyńska-Sejda K (2023) Solvent extraction as a method of recovery and separation of platinum group metals. Materials 16(13):4681. https://doi.org/10.3390/ma16134681
17. Coman C, Mihailescu M, Negrea A, Giannin M, Ciopec M, Duteanu N, Negrea P, Minzatu V (2020) Estimation on fixed-bed column parameters of breakthrough behaviors for gold recovery by adsorption onto modified/functionalized Amberlite XAD7. Int J Environ Res Public Health 17(18):6868. https://doi.org/10.3390/ijerph17186868
18. Volfová L, Mihailescu M, Negrea A, Giannin M, Duteanu N, Ciopec M, Negrea P (2021) Batch and fixed-bed column studies on palladium recovery from acidic solution by modified $MgSiO_3$. Materials 14(4):1003. https://doi.org/10.3390/ma14041003
19. Dlamini ML, Bhaumik M, Pillay K, Maity A (2021) Polyaniline nanofibers, a nanostructured conducting polymer for the remediation of methyl orange dye from aqueous solutions in fixed-bed column studies. Heliyon 7(10):e08180. https://doi.org/10.1016/j.heliyon.2021.e08180
20. Patel H (2021) Comparison of batch and fixed bed column adsorption: a critical review. Int J Environ Sci Technol. https://doi.org/10.1007/s13762-021-03492-y
21. Benettayeb A, Seihoub FZ, Pal P, Ghosh S, Usman M, Chia CH, Usman M, Sillanpää M (2023) Chitosan nanoparticles as potential nano-sorbent for removal of toxic environmental pollutants. Nanomaterials 13(3):447. https://doi.org/10.3390/nano13030447
22. Chowdhury ZZ, Hamid SBA, Zain SM (2014) Evaluating design parameters for breakthrough curve analysis and kinetics of fixed bed columns for Cu (II) cations using lignocellulosic wastes. Bioresour 10(1):732–749. https://doi.org/10.15376/biores.10.1.732-749
23. Elavarasi S, Runtti H, Kangas T, Pesonen J, Lassi U, Tuomikoski S (2022) Column adsorption studies for the removal of ammonium using Na-zeolite-based geopolymers. Resources 11(12):119. https://doi.org/10.3390/resources11120119
24. El Mouhri G, Merzouki M, Belhassan H, Miyah Y, Amakdouf H, Elmountassir R, Lahrichi A (2020) Continuous adsorption modeling and fixed bed column studies: adsorption of tannery wastewater pollutants using beach sand. J Chem 2020:1–9. https://doi.org/10.1155/2020/7613484
25. Malik DS, Jain CK, Yadav AK (2018) Heavy metal removal by fixed-bed column – a review. ChemBioEng Rev 5(3):173–179. https://doi.org/10.1002/cben.201700018
26. Mphahlele MRR, Mosai AK, Tutu H, Kotzé IA (2024) Advancements in sustainable platinum and palladium recovery: unveiling superior adsorption efficiency and selectivity with a novel silica-anchored acylthiourea adsorbent. RSC Adv 14(11):7507–7516. https://doi.org/10.1039/d3ra08169a
27. Mphahlele MRR, Mosai AK, Tutu H, Kotzé IA (2025) Enhanced platinum and palladium recovery from aqueous solutions: a comparative study of the acylthiourea and amine-based silica gel adsorbents. RSC Adv 15:4607–4618. https://doi.org/10.1039/D4RA07935C
28. Ahmed MJ, Hameed BH (2018) Removal of emerging pharmaceutical contaminants by adsorption in a fixed-bed column: a review. Ecotoxicol Environ Saf 149:257–266. https://doi.org/10.1016/j.ecoenv.2017.12.012
29. Patel H (2019) Fixed-bed column adsorption study: a comprehensive review. Appl Water Sci 9(3):1–11. https://doi.org/10.1007/s13201-019-0927-7
30. Ensar O (2017) Fixed-bed column studies on the removal of Fe^{3+} and neural network modelling. Arab J Chem 10(3):313–320. https://doi.org/10.1016/j.arabjc.2014.10.008
31. Lin X, Chen X, Qi G, Shi S, Xiong L, Huang CC, Chen X, Li H (2017) Estimation of fixed-bed column parameters and mathematical modelling of breakthrough behaviours for adsorption of levulinic acid from aqueous solution using SY-01 resin. Sep Purif Technol 174:222–231. https://doi.org/10.1016/j.seppur.2016.10.016
32. Barros D (2013) General aspects of aqueous sorption process in fixed beds. In: Mass transfer—advances in sustainable energy and environment oriented Numerical modeling. IntechOpen. https://doi.org/10.5772/51954
33. Leudjo TA, Klink MJ, Yangkou MX, Naidoo EB (2021) Chitosan nanocomposites for water treatment by fixed-bed continuous flow column adsorption: a review. Carbohydr Polym 255:117398. https://doi.org/10.1016/j.carbpol.2020.117398
34. Naboulsi A, Bouzid B, Grich A, Regti A, El Himri M, El Haddad M (2024) Understanding the column and batch adsorption mechanism of pesticide 2,4,5-T utilizing alginate-biomass hydrogel capsule: a computational and economic investigation. Int J Biol Macromol 275:133762. https://doi.org/10.1016/j.ijbiomac.2024.133762
35. Abin-Bazaine AA, Olmos-Marquez MA, Campos-Trujillo A (2024) A fixed-bed column sorption: breakthrough curves modeling. IntechOpen eBooks. https://doi.org/10.5772/intechopen.1004446
36. López-Cervantes J, Sánchez-Machado DI, Sánchez-Duarte RG, Correa-Murrieta MA (2018) Study of a fixed-bed column in the adsorption of an azo dye from an aqueous medium using a chitosan–glutaraldehyde biosorbent. Adsorpt Sci Technol 36(1–2):215–232. https://doi.org/10.1177/0263617416688021
37. Negrea A, Mihailescu M, Mosoarca G, Ciopec M, Duteanu N, Negrea P, Minzatu V (2020) Estimation on fixed-bed column parameters of breakthrough behaviors for gold recovery by adsorption onto modified/functionalized Amberlite XAD7. Int J Environ Res Public Health 17(18):6868. https://doi.org/10.3390/ijerph17186868
38. Rafati L, Ehrampoush MH, Rafati AA, Mokhtari M, Mahvi AH (2019) Fixed bed adsorption column studies and models for removal of ibuprofen from aqueous solution by strong adsorbent nano-clay composite. J Environ Health Sci Eng 17(2):753–765. https://doi.org/10.1007/s40201-019-00392-9

39. Halim AA, Aziz HA, Johari MAM, Ariffin KS, Adlan MN (2010) Ammoniacal nitrogen and COD removal from semi-aerobic landfill leachate using a composite adsorbent: fixed bed column adsorption performance. J Hazard Mater 175(1–3):960–964. https://doi.org/10.1016/j.jhazmat.2009.10.103
40. Song ST, Hau YF, Saman N, Johari K, Cheu SC, Kong H, Mat H (2016) Process analysis of mercury adsorption onto chemically modified rice straw in a fixed-bed adsorber. J Environ Chem Eng 4(2):1685–1697. https://doi.org/10.1016/j.jece.2016.02.033
41. Liu Z, Mills EC, Mohseni M, Barbeau B, Bérubé PR (2022) Biological ion exchange as an alternative to biological activated carbon for natural organic matter removal: impact of temperature and empty bed contact time (EBCT). Chemosphere 288:132466. https://doi.org/10.1016/j.chemosphere.2021.132466
42. Kanematsu M, Young TM, Fukushi K, Green PG, Darby JL (2012) Individual and combined effects of water quality and empty bed contact time on As (V) removal by a fixed-bed iron oxide adsorber: implication for silicate precoating. Water Res 46(16):5061–5070. https://doi.org/10.1016/j.watres.2012.06.047
43. Bernardis FL, Grant RA, Sherrington DC (2005) A review of methods of separation of the platinum-group metals through their chloro-complexes. React Funct Polym 65(3):205–217. https://doi.org/10.1016/j.reactfunctpolym.2005.05.011
44. Chowdhury S, Saha PD (2012) Batch and continuous (fixed-bed column) biosorption of Cu(II) by *Tamarindus indica* fruit shell. Korean J Chem Eng 30(2):369–378. https://doi.org/10.1007/s11814-012-0127-8